Title
A 2-Pyridone-Amide Inhibitor Targets the Glucose Metabolism Pathway of Chlamydia trachomatis

Journal
mBio, 6(1)

ISSN
2161-2129

Authors
Engström, Patrik
Krishnan, K Syam
Ngyuen, Bidong D
et al.

Publication Date
2015-02-27

DOI
10.1128/mbio.02304-14

Peer reviewed

RESEARCH ARTICLE

A 2-Pyridone-Amide Inhibitor Targets the Glucose Metabolism Pathway of *Chlamydia trachomatis*

Patrik Engström,[a,b,c,g] K. Syam Krishnan,[c,d] Bidong D. Nguyen,[e] Erik Chorell,[c,d] Johan Normark,[a,b,c] Jim Silver,[a] Robert J. Bastidas,[e] Matthew D. Welch,[g] Scott J. Hultgren,[f] Hans Wolf-Watz,[a,b,c] Raphael H. Valdivia,[e] Fredrik Almqvist,[c,d] Sven Bergström[a,b,c]

Department of Molecular Biology, Umeå University, Umeå, Sweden[a]; Laboratory for Molecular Infection Medicine Sweden (MIMS), Umeå University, Umeå, Sweden[b]; Umeå Centre for Microbial Research (UCMR), Umeå University, Umeå, Sweden[c]; Department of Chemistry, Umeå University, Umeå, Sweden[d]; Department of Molecular Genetics and Microbiology, Center for Microbial Pathogenesis, Duke University Medical Center, Durham, North Carolina, USA[e]; Department of Molecular Microbiology and Center for Women's Infectious Disease Research, Washington University School of Medicine, St. Louis, Missouri, USA[f]; Department of Molecular and Cell Biology, University of California, Berkeley, Berkeley, California, USA[g]

K.S.K. and B.D.N. contributed equally to this work.

ABSTRACT **In a screen for compounds that inhibit infectivity of the obligate intracellular pathogen *Chlamydia trachomatis*, we identified the 2-pyridone amide KSK120. A fluorescent KSK120 analogue was synthesized and observed to be associated with the *C. trachomatis* surface, suggesting that its target is bacterial. We isolated KSK120-resistant strains and determined that several resistance mutations are in genes that affect the uptake and use of glucose-6-phosphate (G-6P). Consistent with an effect on G-6P metabolism, treatment with KSK120 blocked glycogen accumulation. Interestingly, KSK120 did not affect *Escherichia coli* or the host cell. Thus, 2-pyridone amides may represent a class of drugs that can specifically inhibit *C. trachomatis* infection.**

IMPORTANCE ***Chlamydia trachomatis* is a bacterial pathogen of humans that causes a common sexually transmitted disease as well as eye infections. It grows only inside cells of its host organism, within a parasitophorous vacuole termed the inclusion. Little is known, however, about what bacterial components and processes are important for *C. trachomatis* cellular infectivity. Here, by using a visual screen for compounds that affect bacterial distribution within the chlamydial inclusion, we identified the inhibitor KSK120. As hypothesized, the altered bacterial distribution induced by KSK120 correlated with a block in *C. trachomatis* infectivity. Our data suggest that the compound targets the glucose-6-phosphate (G-6P) metabolism pathway of *C. trachomatis*, supporting previous indications that G-6P metabolism is critical for *C. trachomatis* infectivity. Thus, KSK120 may be a useful tool to study chlamydial glucose metabolism and has the potential to be used in the treatment of *C. trachomatis* infections.**

Received 12 November 2014 **Accepted** 25 November 2014 **Published** 30 December 2014

Citation Engström P, Krishnan S, Ngyuen BD, Chorell E, Normark J, Silver J, Bastidas RJ, Welch MD, Hultgren SJ, Wolf-Watz H, Valdivia RH, Almqvist F, Bergström S. 2015. A 2-pyridone-amide inhibitor targets the glucose metabolism pathway of *Chlamydia trachomatis*. mBio 6(1):e02304-14. doi:10.1128/mBio.02304-14.

Editor Julian E. Davies, University of British Columbia

Address correspondence to Fedrik Almqvist, Fredrik.almqvist@chem.umu.se, or Sven Bergstrom, Sven.bergstrom@molbiol.umu.se.

Chlamydia trachomatis is the causative agent of many sexually transmitted diseases (1), as well as of trachoma, a chronic eye infection (2). Without antibiotic treatment, *C. trachomatis* infections of the female genital tract can lead to infertility, a major public health concern (3). Although chlamydial infections are treatable with currently available antibiotics, treatment failures occur (4) and there is evidence for lateral transmission of antibiotic resistance in *Chlamydia* species of veterinary importance (5). Potential alternative antichlamydial treatment strategies may include compounds that target specific virulence factors to limit bacterial proliferation and prevent disease while avoiding disruption of the normal bacterial flora (6–8). Such strategies may help reduce the development of resistance to classical antibiotics.

Chlamydia spp. are difficult to study because of their obligate intracellular lifestyle, and methods for routine molecular genetic manipulation of this organism are in their infancy. Chemical genetics provides an alternative approach to study *Chlamydia* spp., and other, less-tractable microbial pathogens, by allowing temporal and quantitative control of the function of a gene product through the use of small molecules (9). Such molecules can provide novel insights into molecular mechanisms of virulence and can also serve as candidates for the design of better therapeutics.

Chlamydiae have a distinctive developmental cycle that involves a transition between two forms. The elementary body (EB) is the infectious form that attaches to and invades target epithelial cells. The EB then transitions to a reticulate body (RB) form, which proliferates within the expanding parasitophorous vacuole, termed the inclusion (10). Midway through the intracellular cycle, RBs begin to transition back to the infectious EB form and are eventually released to the surrounding milieu to infect new host cells (11, 12).

In this study, we conducted a visual screen to identify 2-pyridone inhibitors that impaired *C. trachomatis* infectivity. From this screen, compound KSK120 was identified, and after selection and isolation of KSK120-resistant strains, resistance point mutations were mapped to genes involved in glucose-6-phosphate metabolism.

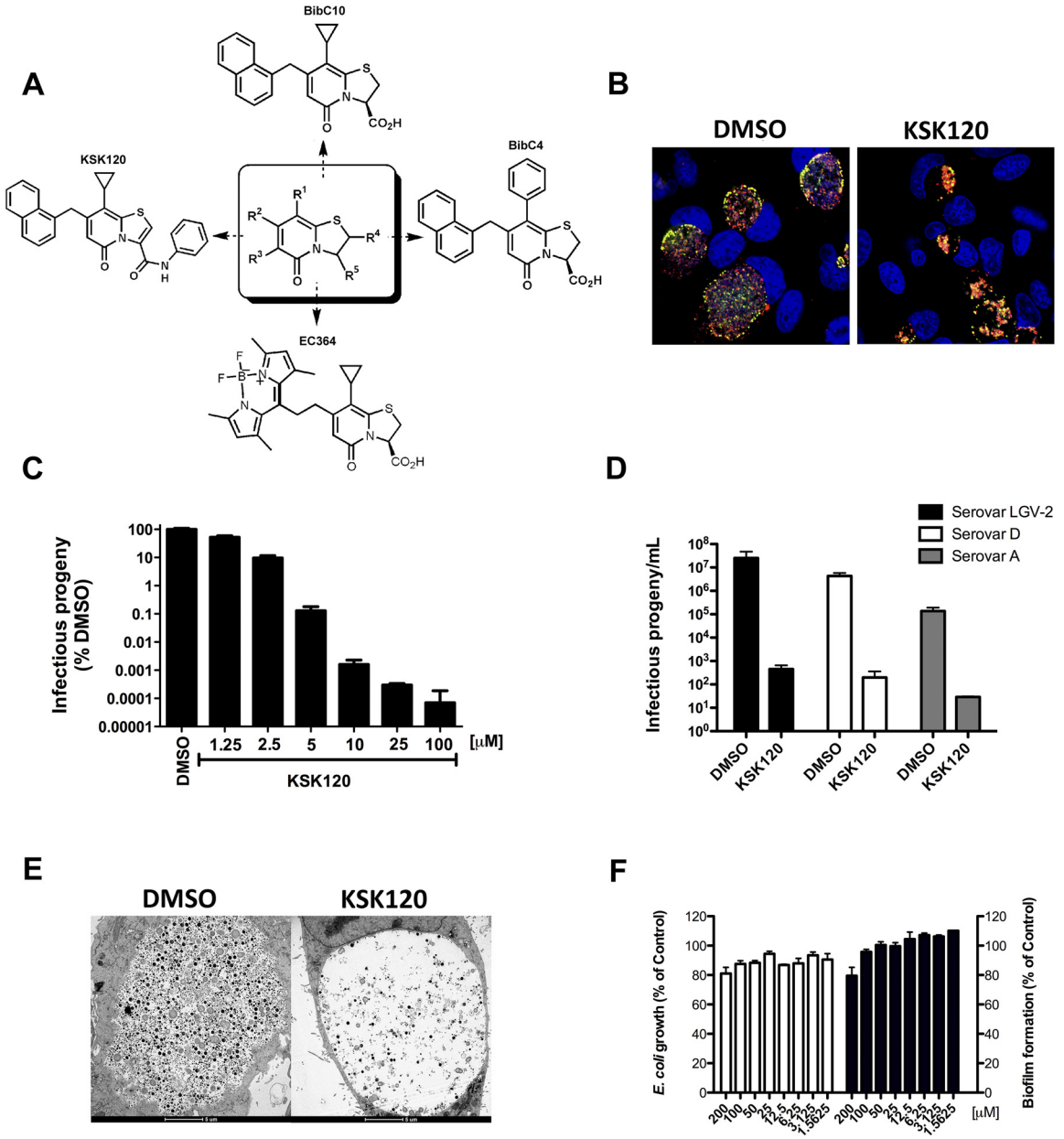

FIG 1 Compound KSK120 has selective anti-*C. trachomatis* activity that blocks its infectivity. (A) Compounds synthesized with substituent variations decorating the 2-pyridone central scaffolds. See Table S1 in the supplemental material for a complete list of compounds tested. (B) HeLa cells infected with *C. trachomatis* serovar LGV-2 were treated for the entire infection with 10 μM KSK120 or DMSO, fixed with methanol at 44 hour postinfection (hpi), and stained with primary antibodies toward major outer membrane protein (MOMP) (red) and heat shock protein 60 (Hsp60) (green). DAPI was used to detect bacterial and host DNA (blue). Confocal laser scanning microscopy was used to obtain the images. (C) HeLa cells infected with *C. trachomatis* LGV-2 were treated with KSK120 or DMSO, and at 44 hpi, infectious progeny were collected for reinfection of new HeLa cells. DMSO treatment results were set to a value of 100. Data presented were acquired from an experiment performed in triplicate. (D) Generation of infectious EB (elementary body) progeny of indicated *C. trachomatis* serovars in the presence of 10 μM KSK120 (44 hpi) or the corresponding amount of DMSO. Presented data are the means of the results of three experiments. (E) Representative transmission electron micrographs of cells infected with *C. trachomatis* LGV-2 treated with 10 μM KSK120 or the corresponding amount of DMSO (44 hpi). (F) Growth and biofilm formation in the presence of KSK120. Results were quantified relative to nontreated *E. coli* results. Representative experiments were performed in triplicate. In all figures, error bars indicate standard deviations (SD).

RESULTS AND DISCUSSION

Compound KSK120 blocks *C. trachomatis* infectivity. On the basis of previous observations that 2-pyridone carboxylic acids can block biofilm formation of *E. coli* (13, 14), as well as our recent findings showing that 2-pyridones have the ability to block infection of the human intracellular pathogen *Listeria monocytogenes* (unpublished observation), we were prompted to investigate a potential effect on chlamydial infectivity. Therefore, we screened a library of 61 2-pyridone compounds with various substitutions around a 2-pyridone central scaffold (Fig. 1A; see also Table S1 in the supplemental material) for their ability to affect intracellular infection by *C. trachomatis* serovar LGV-L2. To identify com-

pounds that inhibit the production of infectious progeny, we assessed each compound for its effect on bacterial distribution within the inclusion. We chose this assay because we previously found that salicylidene acylhydrazide compounds, which cause a reduction in the yields of infectious progeny, alter the normally homogeneous distribution of bacteria within the inclusion to a nonuniform and patchy distribution (15). Each compound, or a dimethyl sulfoxide (DMSO) control, was added to HeLa cells immediately after infection, and the distribution of bacteria within inclusions was assessed at 44 h postinfection (hpi) using confocal fluorescence microscopy. As expected, bacteria were homogenously dispersed inside the inclusions of DMSO-treated control cells (Fig. 1B, left). In contrast, 3 compounds caused bacteria to be heterogeneously dispersed, whereas 8 compounds caused moderate heterogeneous dispersion and 12 were toxic to HeLa cells (see Table S1). The remaining compounds had no effects on either *C. trachomatis* distribution or the host cell.

We determined that large (e.g., phenyl) substituents in position R^1 had low activity (Fig. 1A, BibC4) whereas the smaller cyclopropyl substituent in position R^1 resulted in compounds with moderate activity that caused moderate heterogeneous bacterial dispersion (e.g., BibC10; Fig. 1A). To improve the antichlamydial activity of these compounds and to gain insight into the structure-activity relationships, a small collection of 2-pyridones were synthesized that retained cyclopropyl substitutions in position R^1 but differed in the substitutions at position R^5 (Fig. 1A). Of these, the KSK120 aryl amide derivative showed more activity than the BibC10 parent compound in the bacterial dispersion assay (Fig. 1B, right; see also Table S2 in the supplemental material), whereas all other analogues showed lower activity or were toxic to the host cell.

To verify that heterogeneous bacterial dispersion within inclusions induced by KSK120 correlated with a reduction in levels of infectious progeny, we collected lysates from infected HeLa cells at 44 hpi and assessed the generation of infectious EB progeny by determining the number of inclusion-forming units (IFUs). KSK120 almost completely blocked the generation of IFUs at concentrations of 10 μM and higher, with a 50% effective concentration (EC_{50}) of 1.25 μM (Fig. 1C). We next investigated the effect of KSK120 on different *C. trachomatis* serovars that cause a range of human diseases, including invasive lymphogranuloma venereum (LGV-2 serovar), urogenital infections (serovar D), and trachoma (serovar A). Treatment with 10 μM KSK120 nearly completely blocked infectivity of all the three serovars, with ~10,000-fold-fewer infectious EB progeny compared to the results seen with DMSO-treated cells (Fig. 1D). Furthermore, inclusions in LGV-2-infected cells treated with KSK120 contained reduced numbers of RBs and EBs, although the remaining RBs and EBs were morphologically similar in shape and size to those in untreated cells as determined by transmission electron microscopy (Fig. 1E). Furthermore, 50 μM KSK120 did not affect the growth of uninfected HeLa cells over a period of 48 h as assessed using a colorimetric tetrazolium salt (XTT) cell proliferation assay (98.84% $\pm$ 2.35% proliferation compared with HeLa cells grown in the absence of KSK120), indicating that KSK120 has negligible host cell toxicity.

It was previously shown that a carboxylic acid in position R^5 of 2-pyridones is critical for inhibition of *E. coli* biofilm formation (16). We consistently observed that KSK120, which lacks the carboxylic acid, was unable to inhibit biofilm formation. In addition, KSK120 did not inhibit growth of *E. coli* (Fig. 1F), indicating that this compound does not generally affect bacterial physiology. Thus, KSK120 showed selective antichlamydial activity with limited host cell toxicity, and we focused on it as a primary lead inhibitor for further investigations.

KSK120 associates with the surface of *C. trachomatis* LGV-2. Fluorescent analogues of small-molecule inhibitors can be helpful tools to identify their corresponding molecular targets (17) and to determine whether the primary target resides in the bacteria themselves or in the host cell. Thus, we designed a fluorescent analogue (EC364) by introducing a boron-dipyrromethene (BODIPY) fluorophore into the molecule (Fig. 1A). The antichlamydial effect of EC364 in *C. trachomatis* LGV-2 was indistinguishable from that of KSK120, with bacteria heterogeneously dispersed inside the inclusion of treated cells (see Table S1 in the supplemental material) and a sharp drop in the generation of infectious progeny (see Fig. S1A).

To determine the target of EC364 in *C. trachomatis*, infected cells were treated at 18 hpi with EC364, fixed at 44 hpi, and immunostained with antibodies against the *Chlamydia* major outer membrane protein (MOMP). EC364 associated mostly with bacteria in inclusions (see Fig. S1B in the supplemental material). However, it was not possible to unambiguously assess the location of staining within bacteria due to the small size of RBs. To circumvent this limitation, we employed a standard method, penicillin-G treatment, to induce the enlargement of RBs (18). In penicillin-G-treated *C. trachomatis*, EC364 clearly localized to distinct puncta at the bacterial surface (Fig. 2). Moreover, EC364 suppressed the enlargement of penicillin-G-treated *C. trachomatis* when administered at 18 hpi (Fig. 2, middle row), possibly indicating that these compounds interfere with acquisition of building blocks required for RB enlargement in response to penicillin-G treatment. All together, these data indicate that KSK120 binds to a surface component(s) expressed in the RB form of *C. trachomatis* that is essential for RBs to become infectious EBs.

Compound KSK120 affects G-6P metabolism in *C. trachomatis*. We next sought to identify potential pathways targeted by KSK120 by isolating *Chlamydia* variants that are resistant to the compound. This was accomplished by growing our wild-type *C. trachomatis* LGV-2 strain in the presence of KSK120 for multiple passages (Fig. 3A). Notably, prior KSK120 selection, our wild-type *C. trachomatis* population had been passaged >20 times in the laboratory and only one allelic variant in the *uhpC* gene was identified by genome sequencing at a frequency of 10%, suggesting that spontaneous mutations do not accumulate without selective pressures. After growing the wild type in the presence of KSK120 for 15 passages, we sequenced the genomes of two clonal plaque-purified KSK120-resistant strains and compared them to the reference genome of LGV-2 (GenBank accession number NC_010287) (19). Each strain contained the same four missense mutations. Two were in *uhpC* (CTL0806; accession number YP_001654877.1), which encodes the inner membrane hexose-phosphate (G-6P) transporter UhpC (20) (nucleotide changes G945T and G1285A, causing amino acid substitutions M315I and L429I, the latter of which was also present in a subpopulation at the start of the selection). The third was in gene *efp* (CTL0121; accession number YP_001654212.1), encoding elongation factor P, or E-FP (nucleotide changes C391T, causing amino acid substitution R131C). The fourth was in *rpoC* (CTL0566; accession number YP_001654642.1), encoding RpoC, the RNA polymerase beta prime subunit (nucleotide change C3680A, causing amino

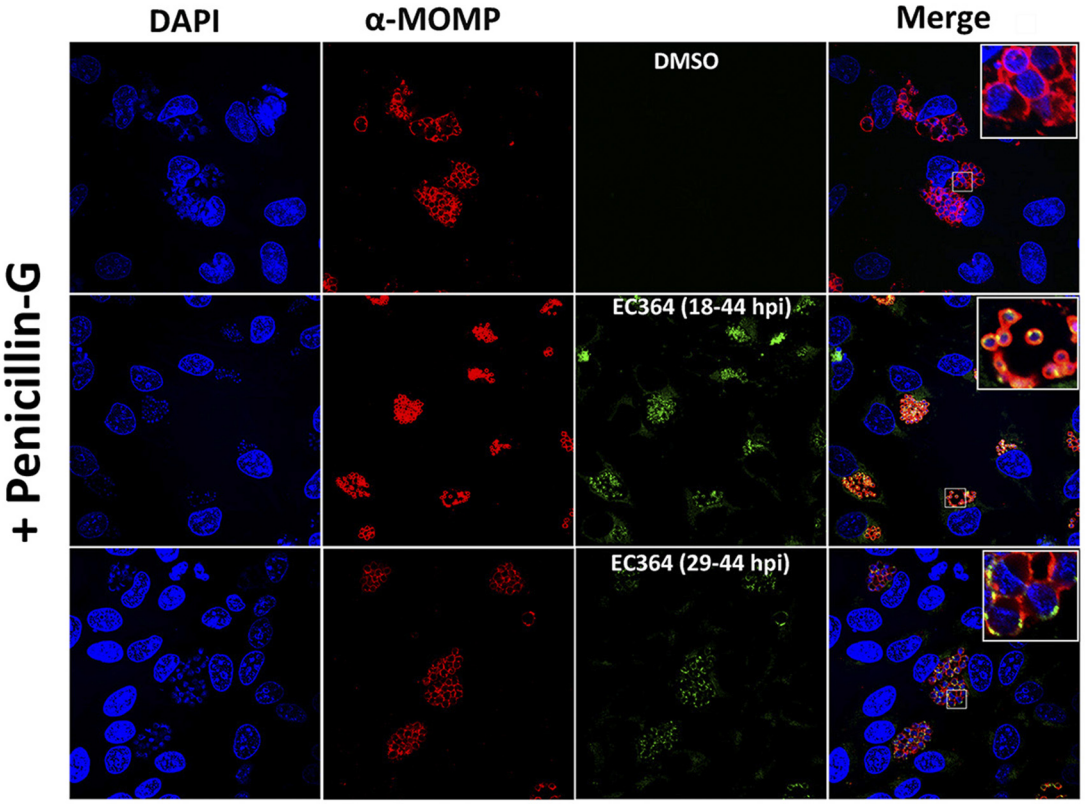

FIG 2 A fluorescent analogue of KSK120 (EC364) associates with surfaces of penicillin-G-treated *C. trachomatis* LGV-2. Penicillin-G (100 U/ml) was added to all infected cells at 18 hpi, concomitant with DMSO treatment (upper panels) or EC364 treatment (100 μM) (middle panels). EC364 treatment was also initiated at 29 hpi (lower panels). At 44 hpi, infected cell were fixed with methanol and stained with primary antibody toward MOMP (red). DAPI was used to detect bacterial and host DNA (blue). Confocal laser scanning microscopy was used to obtain images. DMSO-treated infections were used to define the background.

acid substitution C1224F). We also genotyped four additional clonal KSK120-resistant strains and found that three of them contained all four mutations (in total, 5 strains with this genotype were found), whereas one lacked the mutation in *efp*.

To reveal the order in which the mutations arose during selection, we estimated the percentage of bacteria in the population with each mutant genotype at each passage (Fig. 3B). We determined that the UhpC^{L429I} substitution was selected from the initial inoculum whereas the other alleles appeared in the population starting at passage 8 and increased in abundance over time. To distinguish whether these mutations arose sequentially in a single strain or separately in multiple strains, we performed a plaque purification and genotyped 27 strains from passage 9. We found that individual strains contained mutations in *uhpC* or *efp* but not in both genes (see Table S3 in the supplemental material). Mutations in *rpoC* were not detected. This suggests that each mutation arose in a separate strain and later merged into a single strain containing all four mutations, possibly by horizontal gene transfer. As described below, this approach also allowed us to separate individual strains bearing unique combinations of the identified mutations (Table 1) for further characterization.

To gain further insight into the classes of mutations that can confer KSK120 resistance, we initiated a second independent selection for resistant mutants, starting with a clonal plaque-purified wild-type strain that lacks any mutation in *uhpC*. We grew this strain in the presence of increasing concentrations of KSK120 for 10 passages and then sequenced the genome of a mixed population of resistant variants (Fig. 3C). We identified mutations in two genes. One was in *pgi*, encoding G-6P–isomerase (CTL0633; accession number YP_001654706.1) (nucleotide change A1133C, causing amino acid substitution H378P), an enzyme that catalyzes the first step of glycolysis in *C. trachomatis* (21). The second mutation was in *recC* (CTL0008; accession number YP_001654099.1), encoding exodeoxyribonuclease V gamma chain (nucleotide change C1474A, M415I substitution). The percentages of bacteria in the population with each mutant genotype were 45% for the mutation in *pgi* and 19% for that in *recC*, suggesting the presence of additional rare mutations in the population. Next, we plaque purified and genotyped five clonal strains from passage 10 and determined their genotypes at *pgi* and *recC* as well as at *uhpC*, *efp*, and *rpoC*, since mutations in these genes had been observed during previous selections (Fig. 3A). In these clonal isolates, three strains contained the Pgi^{H378P} substitution, one contained the RecC^{M415I} substitution, and one contained a new mutation in *uhpC* (nucleotide change G1180A, UhpC^{A394T}) (Fig. 3C). To determine which mutations would persist in the population, we allowed further growth for 6 passages in the presence of KSK120. We observed that the mutations in *pgi* and *recC* disappeared and the UhpC^{A394T} variant emerged as the single predominant substitution (Fig. 3D). These data strongly suggest that the majority of KSK120-resistant mutations arise in genes in-

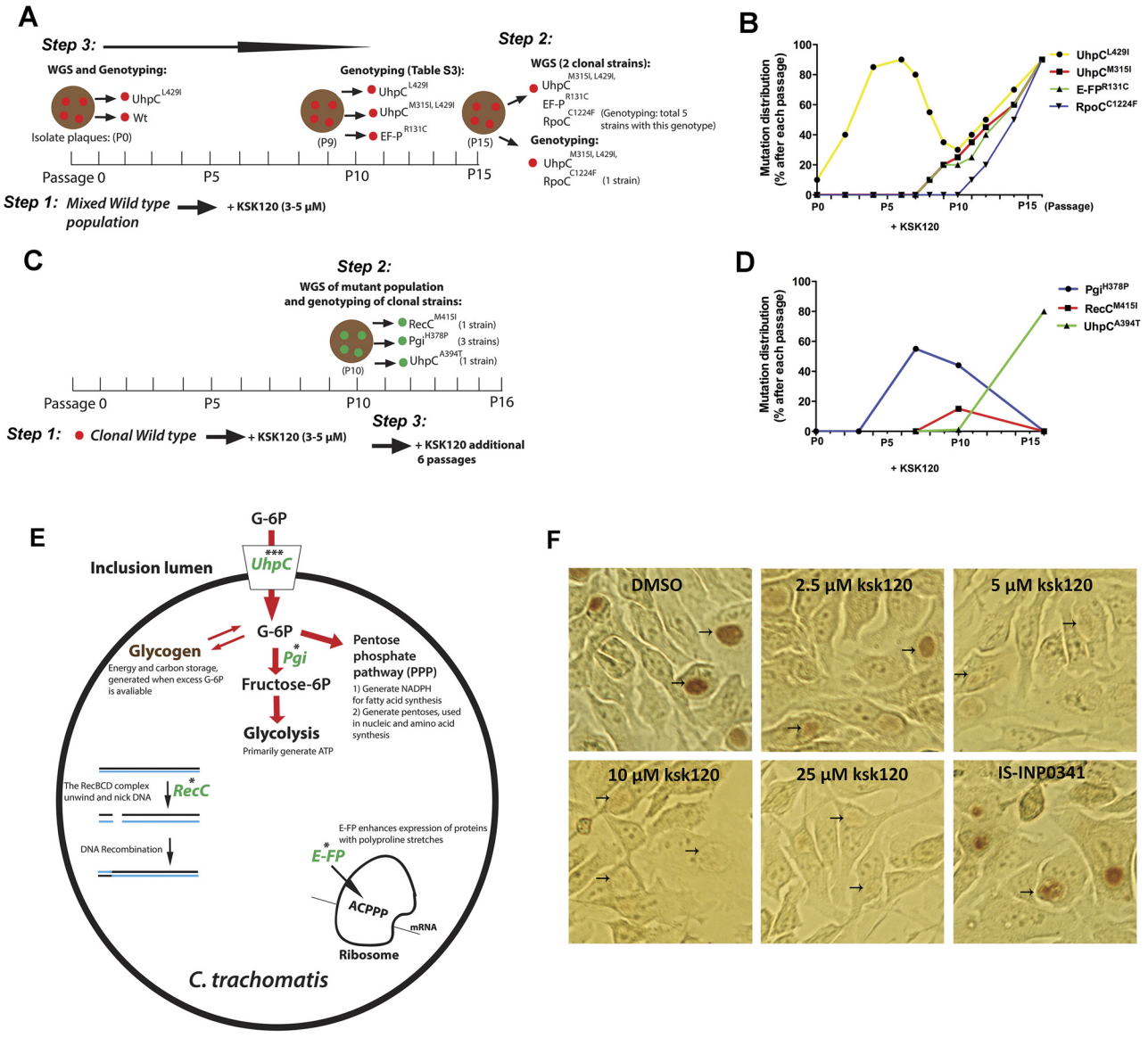

FIG 3 KSK120 affects G-6P metabolic processes of *C. trachomatis*. (A and C) Schemes showing at which mutant passages clonal strains were collected for whole-genome sequencing (WGS) and/or genotyping in the respective selections. Wt, wild type. (A) First selection. (C) Second selection. (B and D) DNA was isolated from mutant passages (bacterial populations), and the respective mutated regions were PCR amplified and subsequently genotyped by capillary sequencing. Mutation frequencies were estimated from obtained chromatogram peak values. Peak values below 10% were omitted. (E) Bacterial pathways and processes in which KSK120-resistant mutations were identified. G-6P metabolic processes and downstream function are based on information from reference 28, the function of E-FP is based on information from references 38 and 39, and RecC data are based on information from reference 40. Mutated proteins are indicated in green, and the stars shown above the respective proteins indicate how many different substitutions were identified from the mutant selections. The mutation in *rpoC* increased KSK120 resistance only slightly (Table 1); therefore, RpoC was excluded from this figure. (F) *C. trachomatis* LGV-2-infected cells were grown in the presence of the indicated compound and at 36 hpi were stained with iodine solution for detection of glycogen. IS-INP0341 is an abbreviation for "iron-saturated INP0341." Treatment with IS-INP0341 was included as a specificity control because this compound inhibits the generation of infectious EB progeny in a manner identical to that of treatment with 5 μM KSK120. Arrows indicate *C. trachomatis* inclusions.

volved in G-6P metabolic processes and that KSK120 likely affects this metabolic circuit.

To verify that the isolated mutant strains are KSK120 resistant, we quantified differences in the generation of infectious EBs between these mutant strains and wild-type *Chlamydia* organisms after treatment with KSK120 (Table 1). Isogenic strains with a mutation in *uhpC*, *efp*, *pgi*, or *recC* were shown to be directly associated with KSK120 resistance because they produced 20-to-250-fold-higher yields of infectious EBs in the presence of the compound (Table 1). The high incidence of resistance mutations in genes that are directly coupled to G-6P uptake and the first steps of glycolysis (Fig. 3E) suggests that G-6P metabolic processes of *C. trachomatis* are affected by KSK120 treatment.

KSK120 affects glycogen accumulation. To explore the potential inhibitory effect of KSK120 on G-6P uptake and/or metabolism, we assessed the consequences of the presence of the inhibitor for bacterial glycogen levels, as glycogen biosynthesis is activated when excess glucose is available (22) (Fig. 3E). Infected cells were

TABLE 1 Collected clonal *C. trachomatis* strains and their KSK120 susceptibility

Strains with indicated substitution(s)[a]	Fold increase in infectious EBs[b]	Mutant passage (P), parental strain
Wild type	1 (±0.38)	Wild-type population
$UhpC^{L429I}$	18.7 (±1.33)	Wild-type population
$UhpC^{L429I, M315I}$	141 (±19.2)	P9, wild-type population
$UhpC^{A394T}$	205 (±42.65)	P10, clonal wild type
Pgi^{H378P}	74.44 (±17)	P10, clonal wild type
$RecC^{M415I}$	118 (±20.1)	P10, clonal wild type
$EF\text{-}P^{R131C}$	186.83 (±19.61)	P9, wild-type population
$UhpC^{L429I, M315I}$, $RpoC^{C1224F}$	242.52 (±30.38)	P15, wild-type population
$UhpC^{L429I, M315I}$, $RpoC^{C1224F}$, $EF\text{-}P^{R131C}$	169.86 (±23.76)	P15, wild-type population

[a] Isolated by plaque purification, lacking the other identified mutations.
[b] Infectious EB progeny generated (at 44 hpi) in the presence of 10 μM KSK120, normalized to input inclusion-forming units (IFU). The values for the wild type were set to 1. Representative data are from an experiment performed in triplicate ± SD.

treated with KSK120 and stained with iodine, a standard method for detection of glycogen buildup in *C. trachomatis* inclusions (23). KSK120 abolished glycogen accumulation (Fig. 3F), consistent with an inhibitory effect on G-6P uptake and/or metabolism. Similar results were obtained with *C. trachomatis* serovar D (see Fig. S2 in the supplemental material). The EC364 fluorescent compound also reduced glycogen accumulation (see Fig. S3), indicating that this analogue is relevant for showing KSK120 specificity and localization. As a control, we treated cells with iron-saturated INP0341 (IS-INP0341), a compound that is not related to KSK120 and that inhibits *C. trachomatis* development by targeting heme metabolism (15). Although 30 μM IS-INP0341 inhibited the generation of infectious *C. trachomatis* progeny to the same extent as 5 μM KSK120, IS-INP0341 did not affect glycogen accumulation. These data suggest that the effects of KSK120 on G-6P metabolic processes are likely to be specific and not an indirect consequence of its anti-*Chlamydia* activity.

Chemical genetics as a tool to investigate *Chlamydia* infectivity. Chemical genetics is a tool that allows identification of target proteins and precise temporal control over their inhibition (9). Nevertheless, there is a general lack of inhibitory compounds that selectively target pathogens without affecting the normal microbiota. Here, we report the results of a novel visual screen for identifying inhibitory compounds that affect *C. trachomatis* infectivity. This screen identified KSK120, a 2-pyridone amide that specifically affects *C. trachomatis* but not *E. coli* or host cells. Such compounds might be helpful in gaining insights into bacterial factors critical for chlamydial infectivity and may form the basis for developing a new class of antichlamydial drugs (6, 7).

To identify the bacterial target(s) of KSK120, we selected for resistant mutants and, for the first time in *Chlamydia* spp., tracked the acquisition of mutations step by step to monitor microevolutionary trends. From our work and that of others, it is evident that *in vitro* selection results in surprisingly few mutations in a *C. trachomatis* population (15, 24). This allowed us to isolate a panel of strains from intermediate or final selection passages that each contained one mutation or a small number of mutations. Many of these mutations mapped to genes involved in G-6P metabolism, suggesting that this pathway is targeted by KSK120. We believe that similar strategies could be applied to the study of other obligate intracellular bacteria to understand how they adapt to new environments and drugs.

Our data strongly support the notion that glucose metabolism, and G-6P transporter UhpC in particular, is targeted by KSK120. This agrees with previous data that suggest that G-6P metabolic processes are critical for *Chlamydia* infectivity (25–29). Thus, KSK120 may prove useful for studying glucose metabolism in *Chlamydia* spp., and its analogs may also be useful in other intracellular bacteria. Importantly, host G-6P is available only to intracellular bacteria and not to those that reside extracellularly. Thus, KSK120 may represent a new class of drugs that can specifically treat infections of intracellular bacterial pathogens such as *Chlamydia* while leaving the normal bacterial flora unperturbed.

MATERIALS AND METHODS

Synthesis and purification of ring-fused 2-pyridones. Compounds C-10 methyl, C-10 CH_2OH, VAC088, VAB086, VA140, VA142, and VA147 were synthesized according to published procedures (16, 30). All the other compounds, except KSK120, were synthesized by basic hydrolysis of the corresponding methyl ester-substituted 2-pyridones (31, 32).

General synthesis of KSK120. Compound C-10 methyl ester was oxidized by a previously reported method (33), and the product was hydrolyzed using lithium bromide (LiBr) and triethylamine (Et_3N) in acetonitrile/water (98/2). After purification by column chromatography, the product was dissolved in dry dichloromethane and cooled to 0°C. Oxalyl chloride (1.5 Eq) was added dropwise, and the solution was allowed to reach room temperature and stirred for 1 h. After the evaporation of solvent to remove HCl, the residue was redissolved in dichloromethane, followed by the addition of triethylamine (3 Eq) and aniline (2 Eq). The solution was continuously stirred for 4 h and then concentrated and purified by column chromatography on a silica gel (see Text S1 in the supplemental material for the additional chemical experimental procedure details).

Chemicals and ring-fused 2-pyridones. 2-Pyridones and the salicylaldehyde hydrazone INP0341 (34) were dissolved in dimethyl sulfoxide (DMSO; Sigma) to reach a final concentration of 20 mM and stored at room temperature without exposure to light for a maximum of 2 months. Prior to experiments, the compounds were diluted in prewarmed RPMI media. Penicillin-G was dissolved in water to reach a concentration of 80,000 U/ml and filter sterilized (Millipore) (0.22-μm-pore-size filter). Compound INP0341 was iron saturated by mixing equal amounts of compound and $FeCl_3$. The mixture was incubated for 1 h at room temperature before being added to prewarmed RPMI media.

***E. coli* growth and biofilm assays.** *E. coli* clinical isolate UTI89 was statically grown in Luria broth for 24 h at 37°C, and optical density (OD) was measured at a wavelength of 600 nm (OD_{600}). For the biofilm assay, *E. coli* was statically grown in Luria broth for 48 h at 26°C and thereafter stained with crystal violet as already described (13). Absorbance was measured at OD_{600}.

Cell culture, *C. trachomatis* infections, plaque assay, and cell toxicity assay. The HeLa cell line (DSMZ) was grown at 37°C (5% CO_2) in RPMI 1640 (Sigma) supplemented with 10% fetal bovine serum (FBS) (Sigma) and 20 mM HEPES. Vero cells (ATCC) were grown in Dulbecco's

modified Eagle's medium (DMEM) (Gibco/Invitrogen) supplemented with 10% FBS (Sigma) at 37°C (5% CO_2). *Chlamydia trachomatis* serovar LGV-L2 454/Bu (ATCC VR902B), *C. trachomatis* serovar D (a gift from S. Muschiol), and *C. trachomatis* serovar A (ATCC VR571B) were propagated in HeLa cells in the absence of cycloheximide, and elementary bodies was purified as previously described by Caldwell et al. (35) and stored in SPG buffer (0.25 M sucrose, 10 mM sodium phosphate, 5 mM L-glutamic acid). For infection experiments, HeLa cells were infected by *C. trachomatis* diluted in Hanks balanced salt solution (HBSS) (Gibco/Invitrogen) with a multiplicity of infection (MOI) of 0.01 to 1 for 1 h at 37°C (5% CO_2). HBSS was subsequently removed, and complete RPMI media supplemented with the indicated compounds were added to the infected cells. Cycloheximide was excluded in all experiments. Clonal populations were collected by plaque assay as described elsewhere (36). Briefly, Vero cells were infected with 100 to 10 IFUs for 2 h and infected cells were overlaid with an agarose-DMEM overlay. Plaques were collected 10 to 20 days after infection and propagated in HeLa cells. Vero cells, HeLa cells, and *C. trachomatis* strains were negative for mycoplasma infection as determined by a detection kit according to the manufacturer's instructions (Stratagene). Cell viability was analyzed using an XTT cell proliferation kit acquired from ATCC. Compound KSK120 was added in triplicate at a concentration of 50 μM. After 24 and 48 h, the XTT mixture was added to the wells according to the manufacturer's instructions (ATCC) and incubated at 37°C for 2.5 h. Subsequently, the plates were read at 470 nm and 660 nm. The results seen with HeLa cells that proliferated in the absence of the compound were set to a value of 100.

Phenotypic screen and immunofluorescence. Semiconfluent HeLa cells grown on coverslips were infected as described above. The compounds presented in Table S1 in the supplemental material were at first tested at a concentration of 100 μM, and treated infections were observed by light microscopy for 44 h. Treated samples were subsequently fixed with methanol for 5 min, background fluorescent signals was reduced by blocking the samples with 5% bovine serum albumin for at least 1 h, and the samples were thereafter incubated with primary anti-MOMP antibody (a gift from Ken Fields) and primary anti-Hsp60 antibody (Santa Cruz Biotechnology). Next, a lissamine rhodamine sulfonyl chloride (LRSC)-conjugated anti-rabbit antibody was used to detect the MOMP antibody and a fluorescein isothiocyanate (FITC)-conjugated anti-mouse antibody (both from Jackson ImmunoResearch Laboratories) was used to detect the Hsp60 antibody. DNA was stained with 200 nM DAPI (4′,6-diamidino-2-phenylindole). Coverslips were mounted on glass slides with fluorescence mounting media (Dako). Images were obtained by confocal laser scanning microscopy (Nikon Eclipse C1 plus) and processed by the use of Adobe Photoshop software (Adobe Systems Inc.). The effect of the compounds was scored based on the distribution of *C. trachomatis* inside the inclusion, before and after fixation. The heterogeneous bacterial distribution inside the chlamydial inclusion was equivalent to a strong phenotypic effect.

Localization of a KSK120 fluorescent analogue. At 18 hpi, RPMI media were changed to media supplemented with 100 μM of the fluorescent analogue EC364. DMSO was used as a control. At 44 hpi, infected cells were washed twice with phosphate-buffered saline (PBS) and then fixed with methanol or 4% paraformaldehyde and stained with the anti-MOMP antibody and DAPI as described above. Penicillin-G was added at 18 hpi, at a concentration of 100 U/ml, and EC364 was added either concomitantly (18 hpi) or at 29 hpi. Images were obtained and processed as described above.

Determination of *C. trachomatis* infectivity. At the indicated time point, media were completely removed and the infected cells were disrupted with ice-cold sterile water to release infectious EB progeny. Released bacteria were diluted in HBSS, fresh HeLa cells were infected, and the *C. trachomatis* inclusions were counted 30 to 40 h after reinfection. Data are represented as the relative numbers of EBs in treated infections compared to the numbers of EBs in DMSO-treated infections. When multiple strains were analyzed, a titration was performed in parallel to the primary treated infections to calculate the exact number of infectious EB progeny per treated IFU (36).

Glycogen staining. Potassium iodine and iodine (both from Sigma) were dissolved in 100% methanol. Subsequently, an equal amount of glycerol was added to the solution. At time points postinfection, culture media were removed and infected cells were washed once with PBS before incubation in iodine solution for 30 min. Thereafter, the iodine solution was removed and samples were air-dried for 90 min prior to microscopic analysis (37). Samples were visualized using an inverted Nikon Eclipse Ti microscope.

Mutant selections. HeLa cells grown in large flasks were infected with an MOI of 5 (~10^8 IFUs) and treated with a subinhibitory concentration of compound KSK120. From each mutant passage, infectious EB progeny were collected at 44 to 48 hpi and used for reinfection. During the first 4 to 6 passages, the treated bacteria were grown at an MOI of 2 or higher; thereafter, the selection proceeded with an MOI of 2 or lower (preferentially lower than an MOI of 1). From each mutant passage, an aliquot of bacteria was saved for analysis.

WGS and genotyping. *C. trachomatis* genomic DNA prepared for whole-genome sequencing (WGS) was purified from density-gradient-purified bacteria as described above. For WGS, 1 μg of enriched chlamydial DNA was fragmented with an Adaptive Focused Acoustics S220 instrument (Covaris, Inc., Woburn, MA), and DNA sequencing libraries were prepared with a library construction kit (TruSeq DNA sample preparation kit v2; Illumina, Inc., San Diego, CA) according to the manufacturer's instructions. Libraries were sequenced on a MiSeq DNA sequencing platform (Illumina, Inc., San Diego, CA) at the IGSP DNA Core sequencing facility of Duke University. Genome assembly and single nucleotide variant (SNV) identification were performed with Geneious version 6 from Biomatters. The *C. trachomatis* L2 434/Bu genome (GenBank accession no. NC_010287) was used as the reference sequence. A mutation is defined here as a nucleotide variant present at a frequency above 15% and strand bias below 80%, detectable by both WGS and capillary sequencing in a bacterial population. To identify mutations by capillary sequencing, templates from selected regions were amplified by PCR and sequenced by capillary sequencing (Big Dye; Applied Biosystems). The intensity of the fluorescence peaks detected by capillary DNA sequencing was used to estimate the relative abundance of any single nucleotide variant in the bacterial population. Estimated frequencies were consistent with the values obtained from WGS.

Transmission electron microscopy (TEM). At 44 hpi, infected cells were processed for TEM as previously described (36). Briefly, cells were fixed with 2.5% glutaraldehyde–0.05% malachite green–0.1 M sodium cacodylate buffer (pH 6.8) and then postfixed with 0.5% osmium tetroxide–0.8% potassium ferricyanide–0.1 M sodium cacodylate–1% tannic acid–1% uranyl acetate. Samples were dehydrated with graded amounts of ethanol and embedded in Spur resin and were subsequently imaged on a Tecnai G2 Twin microscope (FEI).

SUPPLEMENTAL MATERIAL

Supplemental material for this article may be found at http://mbio.asm.org/lookup/suppl/doi:10.1128/mBio.02304-14/-/DCSupplemental.

Figure S1, TIF file, 2.1 MB.
Figure S2, TIF file, 0.6 MB.
Figure S3, TIF file, 0.6 MB.
Table S1, DOC file, 0.9 MB.
Table S2, DOC file, 0.1 MB.
Table S3, DOC file, 0.03 MB.
Text S1, DOC file, 0.05 MB.

ACKNOWLEDGMENTS

We thank B. Guo and Å. Gylfe for critically reading the manuscript and S. Areljung, I. Nilsson, H. Uvell, and M. Bergström for technical assistance.

We acknowledge funding from the Swedish Research Council (F.A., S.B., and H.W.-W.), the Knut and Alice Wallenberg Foundation (F.A. and S.B.), the Göran Gustafsson Foundation (F.A.), the Swedish Foundation for Strategic Research (F.A.), and NIH funding to R.H.V. and R.J.B. (grant AI100759), S.J.H. (grants AI099099 and AI048689), and M.D.W. (grant AI109044). K.S.K. thanks the JC Kempe Foundation for funding.

E.C. and K.S.K. designed and synthesized 2-pyridone compounds. B.D.N. with the assistance of R.J.B. performed electron microscopy analysis and library construction for genome sequencing and subsequent assembly and analysis. J.S. performed cell toxicity experiments and assisted in some of the microscopic analysis. P.E. planned and executed the rest of the experiments, including compound phenotypic screen, characterize the effect of KSK120, selection and isolation of resistant mutations, microscopic analysis, sample preparation for genome sequencing and subsequent genotyping. H.W.-W., R.H.V., S.B., and F.A. supervised the research. P.E. wrote the paper under the supervision of M.D.W., J.N., R.H.V., S.B., F.A., and S.H. K.S.K. wrote the chemical methods part of the paper.

REFERENCES

1. **Haggerty CL, Gottlieb SL, Taylor BD, Low N, Xu F, Ness RB.** 2010. Risk of sequelae after *Chlamydia trachomatis* genital infection in women. J Infect Dis **201**(Suppl 2):S134–S155. http://dx.doi.org/10.1086/652395.
2. **Burton MJ, Mabey DC.** 2009. The global burden of trachoma: a review. PLOS Negl Trop Dis **3**:e460. http://dx.doi.org/10.1371/journal.pntd.0000460.
3. **Paavonen J, Eggert-Kruse W.** 1999. *Chlamydia trachomatis*: impact on human reproduction. Hum Reprod Update **5**:433–447. http://dx.doi.org/10.1093/humupd/5.5.433.
4. **Somani J, Bhullar VB, Workowski KA, Farshy CE, Black CM.** 2000. Multiple drug-resistant *Chlamydia trachomatis* associated with clinical treatment failure. J Infect Dis **181**:1421–1427. http://dx.doi.org/10.1086/315372.
5. **Borel N, Regenscheit N, Di Francesco A, Donati M, Markov J, Masserey Y, Pospischil A.** 2012. Selection for tetracycline-resistant *Chlamydia suis* in treated pigs. Vet Microbiol **156**:143–146. http://dx.doi.org/10.1016/j.vetmic.2011.10.011.
6. **Nguyen BD, Cunningham D, Liang X, Chen X, Toone EJ, Raetz CR, Zhou P, Valdivia RH.** 2011. Lipooligosaccharide is required for the generation of infectious elementary bodies in *Chlamydia trachomatis*. Proc Natl Acad Sci U S A **108**:10284–10289. http://dx.doi.org/10.1073/pnas.1107478108.
7. **Valdivia RH.** 2012. Thinking outside the box: new strategies for antichlamydial control. Future Microbiol **7**:427–429. http://dx.doi.org/10.2217/fmb.12.25.
8. **Cegelski L, Marshall GR, Eldridge GR, Hultgren SJ.** 2008. The biology and future prospects of antivirulence therapies. Nat Rev Microbiol **6**:17–27. http://dx.doi.org/10.1038/nrmicro1818.
9. **Puri AW, Bogyo M.** 2009. Using small molecules to dissect mechanisms of microbial pathogenesis. ACS Chem Biol **4**:603–616. http://dx.doi.org/10.1021/cb9001409.
10. **Fields KA, Hackstadt T.** 2002. The chlamydial inclusion: escape from the endocytic pathway. Annu Rev Cell Dev Biol **18**:221–245. http://dx.doi.org/10.1146/annurev.cellbio.18.012502.105845.
11. **Todd WJ, Caldwell HD.** 1985. The interaction of *Chlamydia trachomatis* with host cells: ultrastructural studies of the mechanism of release of a biovar II strain from HeLa 229 cells. J Infect Dis **151**:1037–1044. http://dx.doi.org/10.1093/infdis/151.6.1037.
12. **Hybiske K, Stephens RS.** 2007. Mechanisms of host cell exit by the intracellular bacterium *Chlamydia*. Proc Natl Acad Sci U S A **104**:11430–11435. http://dx.doi.org/10.1073/pnas.0703218104.
13. **Pinkner JS, Remaut H, Buelens F, Miller E, Aberg V, Pemberton N, Hedenström M, Larsson A, Seed P, Waksman G, Hultgren SJ, Almqvist F.** 2006. Rationally designed small compounds inhibit pilus biogenesis in uropathogenic bacteria. Proc Natl Acad Sci U S A **103**:17897–17902. http://dx.doi.org/10.1073/pnas.0606795103.
14. **Cegelski L, Pinkner JS, Hammer ND, Cusumano CK, Hung CS, Chorell E, Aberg V, Walker JN, Seed PC, Almqvist F, Chapman MR, Hultgren SJ.** 2009. Small-molecule inhibitors target Escherichia coli amyloid biogenesis and biofilm formation. Nat Chem Biol **5**:913–919. http://dx.doi.org/10.1038/nchembio.242.
15. **Engström P, Nguyen BD, Normark J, Nilsson I, Bastidas RJ, Gylfe A, Elofsson M, Fields KA, Valdivia RH, Wolf-Watz H, Bergström S.** 2013. Mutations in *hemG* mediate resistance to salicylidene acylhydrazides, demonstrating a novel link between protoporphyrinogen oxidase (HemG) and *Chlamydia trachomatis* infectivity. J Bacteriol **195**:4221–4230. http://dx.doi.org/10.1128/JB.00506-13.
16. **Aberg V, Hedenström M, Pinkner JS, Hultgren SJ, Almqvist F.** 2005. C-terminal properties are important for ring-fused 2-pyridones that interfere with the chaperone function in uropathogenic *E. coli*. Org Biomol Chem **3**:3886–3892. http://dx.doi.org/10.1039/b509376g.
17. **Chorell E, Pinkner JS, Bengtsson C, Edvinsson S, Cusumano CK, Rosenbaum E, Johansson LB, Hultgren SJ, Almqvist F.** 2012. Design and synthesis of fluorescent pilicides and curlicides: bioactive tools to study bacterial virulence mechanisms. Chemistry **18**:4522–4532. http://dx.doi.org/10.1002/chem.201103936.
18. **Skilton RJ, Cutcliffen LT, Barlow D, Wang Y, Salim O, Lambden PR, Clarke IN.** 2009. Penicillin induced persistence in *Chlamydia trachomatis*: high quality time lapse video analysis of the developmental cycle. PLoS One **4**:e7723. http://dx.doi.org/10.1371/journal.pone.0007723.
19. **Thomson NR, Holden MT, Carder C, Lennard N, Lockey SJ, Marsh P, Skipp P, O'Connor CD, Goodhead I, Norbertzcak H, Harris B, Ormond D, Rance R, Quail MA, Parkhill J, Stephens RS, Clarke IN.** 2008. *Chlamydia trachomatis*: genome sequence analysis of lymphogranuloma venereum isolates. Genome Res **18**:161–171.
20. **Schwöppe C, Winkler HH, Neuhaus HE.** 2002. Properties of the glucose-6-phosphate transporter from *Chlamydia pneumoniae* (HPTcp) and the glucose-6-phosphate sensor from *Escherichia coli* (UhpC). J Bacteriol **184**:2108–2115. http://dx.doi.org/10.1128/JB.184.8.2108-2115.2002.
21. **Stephens RS, Kalman S, Lammel C, Fan J, Marathe R, Aravind L, Mitchell W, Olinger L, Tatusov RL, Zhao QX, Koonin EV, Davis RW.** 1998. Genome sequence of an obligate intracellular pathogen of humans: *Chlamydia trachomatis*. Science **282**:754–759. http://dx.doi.org/10.1126/science.282.5389.754.
22. **Preiss J.** 1984. Bacterial glycogen synthesis and its regulation. Annu Rev Microbiol **38**:419–458. http://dx.doi.org/10.1146/annurev.mi.38.100184.002223.
23. **Wang Y, Kahane S, Cutcliffe LT, Skilton RJ, Lambden PR, Persson K, Bjartling C, Clarke IN.** 2013. Genetic transformation of a clinical (genital tract), plasmid-free isolate of *Chlamydia trachomatis*: engineering the plasmid as a cloning vector. PLoS One **8**:e59195. http://dx.doi.org/10.1371/journal.pone.0059195.
24. **Borges V, Ferreira R, Nunes A, Sousa-Uva M, Abreu M, Borrego MJ, Gomes JP.** 2013. Effect of long-term laboratory propagation on *Chlamydia trachomatis* genome dynamics. Infect Genet Evol **17**:23–32. http://dx.doi.org/10.1016/j.meegid.2013.03.035.
25. **Iliffe-Lee ER, McClarty G.** 2000. Regulation of carbon metabolism in *Chlamydia trachomatis*. Mol Microbiol **38**:20–30. http://dx.doi.org/10.1046/j.1365-2958.2000.02102.x.
26. **Saka HA, Thompson JW, Chen YS, Kumar Y, Dubois LG, Moseley MA, Valdivia RH.** 2011. Quantitative proteomics reveals metabolic and pathogenic properties of *Chlamydia trachomatis* developmental forms. Mol Microbiol **82**:1185–1203. http://dx.doi.org/10.1111/j.1365-2958.2011.07877.x.
27. **Omsland A, Sager J, Nair V, Sturdevant DE, Hackstadt T.** 2012. Developmental stage-specific metabolic and transcriptional activity of *Chlamydia trachomatis* in an axenic medium. Proc Natl Acad Sci U S A **109**:19781–19785. http://dx.doi.org/10.1073/pnas.1212831109.
28. **Omsland A, Sixt BS, Horn M, Hackstadt T.** 2014. Chlamydial metabolism revisited: interspecies metabolic variability and developmental stage-specific physiologic activities. FEMS Microbiol Rev **38**:779–801.
29. **Sixt BS, Siegl A, Muller C, Watzka M, Wultsch A, Tziotis D, Montanaro J, Richter A, Schmitt-Kopplin P, Horn M.** 2013. Metabolic features of Protochlamydia amoebophila elementary bodies—a link between activity and infectivity in Chlamydiae. PLoS Pathog **9**:e1003553.
30. **Aberg V, Das P, Chorell E, Hedenström M, Pinkner JS, Hultgren SJ, Almqvist F.** 2008. Carboxylic acid isosteres improve the activity of ring-fused 2-pyridones that inhibit pilus biogenesis in *E. coli*. Bioorg Med Chem Lett **18**:3536–3540. http://dx.doi.org/10.1016/j.bmcl.2008.05.020.
31. **Chorell E, Pinkner JS, Bengtsson C, Banchelin TS, Edvinsson S, Linusson A, Hultgren SJ, Almqvist F.** 2012. Mapping pilicide anti-

virulence effect in *Escherichia coli*, a comprehensive structure-activity study. Bioorg Med Chem **20:**3128–3142. http://dx.doi.org/10.1016/j.bmc.2012.01.048.
32. **Pemberton N, Aberg V, Almstedt H, Westermark A, Almqvist F.** 2004. Microwave-assisted synthesis of highly substituted aminomethylated 2-pyridones. J Org Chem **69:**7830–7835. http://dx.doi.org/10.1021/jo048554y.
33. **Chorell E, Das P, Almqvist F.** 2007. Diverse functionalization of thiazolo ring-fused 2-pyridones. J Org Chem **72:**4917–4924. http://dx.doi.org/10.1021/jo0704053.
34. **Dahlgren MK, Zetterström CE, Gylfe S, Linusson A, Elofsson M.** 2010. Statistical molecular design of a focused salicylidene acylhydrazide library and multivariate QSAR of inhibition of type III secretion in the gram-negative bacterium *Yersinia*. Bioorg Med Chem **18:**2686–2703. http://dx.doi.org/10.1016/j.bmc.2010.02.022.
35. **Caldwell HD, Kromhout J, Schachter J.** 1981. Purification and partial characterization of the major outer membrane protein of *Chlamydia trachomatis*. Infect Immun **31:**1161–1176.
36. **Nguyen BD, Valdivia RH.** 2012. Virulence determinants in the obligate intracellular pathogen *Chlamydia trachomatis* revealed by forward genetic approaches. Proc Natl Acad Sci U S A **109:**1263–1268. http://dx.doi.org/10.1073/pnas.1117884109.
37. **Yong DC, Paul NR.** 1986. Micro direct inoculation method for the isolation and identification of *Chlamydia trachomatis*. J Clin Microbiol **23:**536–538.
38. **Doerfel LK, Wohlgemuth I, Kothe C, Peske F, Urlaub H, Rodnina MV.** 2013. EF-P is essential for rapid synthesis of proteins containing consecutive proline residues. Science **339:**85–88. http://dx.doi.org/10.1126/science.1229017.
39. **Ude S, Lassak J, Starosta AL, Kraxenberger T, Wilson DN, Jung K.** 2013. Translation elongation factor EF-P alleviates ribosome stalling at polyproline stretches. Science **339:**82–85. http://dx.doi.org/10.1126/science.1228985.
40. **Handa N, Yang L, Dillingham MS, Kobayashi I, Wigley DB, Kowalczykowski SC.** 2012. Molecular determinants responsible for recognition of the single-stranded DNA regulatory sequence, chi, by RecBCD enzyme. Proc Natl Acad Sci U S A **109:**8901–8906. http://dx.doi.org/10.1073/pnas.1206076109.